



Cite this: *Chem. Sci.*, 2019, 10, 781

All publication charges for this article have been paid for by the Royal Society of Chemistry

Received 3rd October 2018  
Accepted 29th October 2018

DOI: 10.1039/c8sc04385j

rs.c.li/chemical-science

# Mild complexation protocol for chiral Cp<sup>x</sup>Rh and Ir complexes suitable for *in situ* catalysis†

B. Audic,<sup>a</sup> M. D. Wodrich<sup>b</sup> and N. Cramer<sup>\*a</sup>

A practical complexation method for chiral cyclopentadienyl (Cp<sup>x</sup>) iridium and rhodium complexes is described. The procedure uses the free Cp<sup>x</sup>H with stable and commercially available rhodium(i) and iridium(i) salts without base or additive. The conditions are mild and do not require the exclusion of air and moisture. A salient feature is the suitability for *in situ* complexations enhancing the user-friendliness of Cp<sup>x</sup> ligands in asymmetric catalysis. DFT-calculations confirm an intramolecular proton abstraction pathway by either the bound acetate or methoxide. Furthermore, the superior facial selectivity of the proton abstraction step enabled the development of TMS-containing trisubstituted Cp<sup>x</sup> ligands which display improved enantioselectivities for the benchmarking dihydroisoquinolone synthesis.

## Introduction

Cyclopentadienyl (Cp) coordinated transition-metal complexes are a very important class of catalysts enabling a broad range of versatile and atom-economic transformations.<sup>1</sup> During the last decade, the dominance of Cp and Cp\* (pentamethylcyclopentadienyl) has been challenged by new designer Cp ligands. Modulation of the electronic and steric properties of the Cp ligands has become a key focus for reaction optimization. These ligands display superior performance such as enhanced reactivity,<sup>2</sup> improved regioselectivity<sup>3</sup> and diastereoselectivity.<sup>4</sup> Moreover, the rise of chiral Cp ligands (Cp<sup>x</sup>) enabled the development of enantioselective processes.<sup>5</sup>

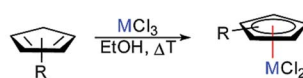
While the synthesis of simple classical Cp\* and Cp complexes with late transition-metals is well established,<sup>6</sup> accessing the corresponding metal Cp complexes of more elaborate – especially chiral – Cp derivatives remains problematic and suffers from a number of undesirable attributes (Fig. 1). For instance, the increased value of tailored cyclopentadienes requiring multi-step syntheses imposes the use of the CpH derivative as the limiting reactant, making protocols that use multiple CpH equivalents prohibitively inefficient. A frequently largely reduced crystallinity and/or enhanced solubility limit purification options of reaction mixtures from suboptimal reaction outcomes. Until now, the most reliably and broadly applicable method involves the use of stoichiometric

amounts of highly toxic thallium bases,<sup>5f</sup> often paired with toxic benzene as solvent.<sup>7</sup> Alkali bases were inferior and caused often complex reaction outcomes. A complementary method used chloride based metal salts without a base.<sup>8</sup> The released hydrochloric acid during the complexation is incompatible with some sensitive functional groups of designer Cp scaffolds. We have developed a complementary complexation strategy capitalizing on β-carbon elimination of cyclopentadienyl carbinols as Cp-ligand precursors.<sup>9</sup> While this method consists of an improvement, it requires the synthesis of the ligand precursor

### Traditional Complexations<sup>6</sup>



- ✓ general
- ✗ toxic thallium base
- ✗ no *in situ* catalysis



- ✓ simple conditions
- ✓ release of HCl
- ✗ not general (fails for Cp<sup>x</sup>)
- ✗ no *in situ* catalysis

### Advanced Complexation Strategies:

#### β-C Elimination<sup>9</sup>



- ✓ *in situ* catalysis
- special precursor
- ✗ limited scope (only hindered CpH's)

#### Addition Across Fulvenes<sup>2g,8b</sup>



- ✓ simple conditions
- special precursor
- ✗ no *in situ* catalysis

#### This work



- ✓ general (2-5-substituted CpH's, chiral CpH's)
- ✓ simple conditions (no exclusion of O<sub>2</sub>, H<sub>2</sub>O)
- ✓ *in situ* catalysis

<sup>a</sup>Laboratory of Asymmetric Catalysis and Synthesis, EPFL SB ISIC LCSA, BCH 4305, CH-1015 Lausanne, Switzerland. E-mail: nicolai.cramer@epfl.ch

<sup>b</sup>Laboratory for Computational Molecular Design, EPFL SB ISIC LCMD, BCH 5312, CH-1015 Lausanne, Switzerland. E-mail: matthew.wodrich@epfl.ch

† Electronic supplementary information (ESI) available: Experimental procedures and characterization of all new compounds. CCDC 1869889, 1869894, 1869888 and 1869893. For ESI and crystallographic data in CIF or other electronic format see DOI: 10.1039/c8sc04385j

Fig. 1 Characteristics and drawbacks of complexation strategies for cyclopentadienyl ligands.



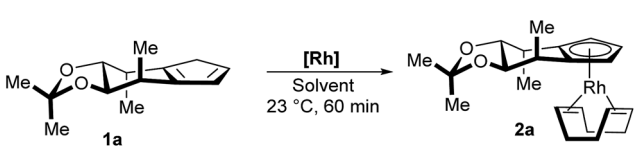
by an additional synthetic step. Moreover, it is limited to highly substituted and hindered Cp variants. In consequence, the development of a robust and general complexation platform for a broad range of tailored chiral Cp<sup>x</sup> ligands remains an important task in improving utility and user friendliness of the resulting Cp metal catalysts.

Herein, we report a mild and convenient method to access key Rh(I) and Ir(I) Cp complexes upon simply mixing a stable and easily accessible metal precursor with Cp<sup>x</sup>H in protic solvents. The protocol qualifies as well for user friendly *in situ* catalyst assembly.

## Results and discussion

We started our investigations towards a mild and general complexation with cyclopentadiene **1a**. A set of common rhodium precursors was screened for reactivity under a variety of conditions and additives (Table 1). The common [Rh(cod)Cl]<sub>2</sub> did not react at all (entries 1 and 2). As well, no reaction was observed for [Rh(cod)OMe]<sub>2</sub> in toluene (entry 3). In contrast, running the reaction in methanol produced the desired Cp complex **2a** in modest yield (entry 4). Switching the rhodium source to [Rh(cod)OAc]<sub>2</sub> resulted in a fast and clean conversion yielding **2a** in 88% yield (entry 5). Ethanol and TFE proved to be as efficient as methanol (entries 6 and 9), whereas bulkier alcohols display largely decreased reaction rate and yields (entries 7 and 8). HFIP mainly led to degradation (entry 10). The use of THF as solvent completely inhibited the reaction (entry 11). Notably, the complexation is user friendly and has low technical requirements. It does not require the use of a glovebox and no precaution to exclude oxygen and humidity from the reaction vessel has to be taken. The final complexes bearing the stabilizing cyclooctadiene (cod) ligand are stable towards convenient standard flash chromatography on silica gel.

Table 1 Optimization of the complexation<sup>a</sup>



Entry	[Rh]	Solvent	Conversion <sup>b</sup> (%)	Yield <sup>b</sup> (%)
1	[Rh(cod)Cl] <sub>2</sub>	toluene	<5	0
2	[Rh(cod)Cl] <sub>2</sub>	MeOH	<5	0
3	[Rh(cod)OMe] <sub>2</sub>	toluene	<5	0
4	[Rh(cod)OMe] <sub>2</sub>	MeOH	85	28 <sup>c</sup>
5	[Rh(cod)OAc] <sub>2</sub>	MeOH	100	88
6	[Rh(cod)OAc] <sub>2</sub>	EtOH	100	89
7	[Rh(cod)OAc] <sub>2</sub>	iPrOH	50	41
8	[Rh(cod)OAc] <sub>2</sub>	<i>t</i> BuOH	10	5
9	[Rh(cod)OAc] <sub>2</sub>	TFE	100	88
10	[Rh(cod)OAc] <sub>2</sub>	HFIP	100	30
11	[Rh(cod)OAc] <sub>2</sub>	THF	<5	0

<sup>a</sup> Conditions: 40 μmol **1a**, 24 μmol [Rh], 0.2 M in indicated solvent at 23 °C for 60 min. <sup>b</sup> Determined by <sup>1</sup>H-NMR with an internal standard. <sup>c</sup> Partial cleavage of the acetal (30%) was observed.

Initially, a variety of achiral cyclopentadiene substrates were tested (Scheme 1). For instance, *t*Bu<sub>2</sub>CpH, Me<sub>4</sub>CpH and Cp<sup>\*</sup>H participated in a smooth and rapid complexation, giving the desired CpRh<sup>I</sup>(cod) complexes **2b–2d** in excellent yields. Solely, bulky and electron-deficient Ph<sub>4</sub>CpH required longer reaction time and gave reduced yields of **2e**. With the observed success for the achiral Cp ligands, we have successfully tested the complete portfolio of the most useful chiral Cp<sup>x</sup> ligands for this transformation. In detail, mannitol-derived Cp ligand **2a**<sup>4f</sup> was isolated in 85% yield. The mild conditions at ambient temperature were compatible with the acetal group. Similarly, readily accessible cyclopentane-fused cyclopentadiene **1f**<sup>9a</sup> and the most versatile methoxy-bearing Cp<sup>x</sup>H **1g**<sup>10</sup> engaged in complexations giving **2f** and **2g** in very high yields. Moderate solubility of the Cp<sup>x</sup>H **2g** required some heating. Bulkier isopropoxy-derivative (**2h**) reacts at ambient temperature, whereas substrates with larger groups (**2i–2j**) require gentle heating for optimal reactivity without compromising the high yield. Bulky tri-substituted cyclopentadiene **1k** gave corresponding complex **2k** in significantly improved yields compared to the thallium-process.<sup>11</sup> Notably, the complexation protocol works as well very smoothly for penta-substituted Cp<sup>x\*</sup> substrate (**2l**). Such true chiral Cp<sup>\*</sup> analogues have been so far refractory substrates for complexation, hampering application in catalysis. Previously, any classical complexation methods failed for this substrate, making β-carbon elimination strategy from *tert*-carbinols the only viable method.<sup>9</sup> Importantly, the illustrated complexation strategy is equally viable to access the corresponding Cp<sup>x</sup>Ir complexes. The complexation employing commercially available [Ir(cod)OMe]<sub>2</sub> complex provided the



Scheme 1 Conditions: 0.1 mmol **1x**, 0.06 mmol [Rh(cod)OAc]<sub>2</sub> or [Ir(cod)OMe]<sub>2</sub> in toluene/MeOH (1 : 1) (0.2 M) at 23 °C. (a) 0.4 mmol **1x**, 0.1 mmol [Rh(cod)OAc]<sub>2</sub>; (b) 24 h; (c) 70 °C; (d) [Ir(cod)OMe]<sub>2</sub> instead of [Rh(cod)OAc]<sub>2</sub>.



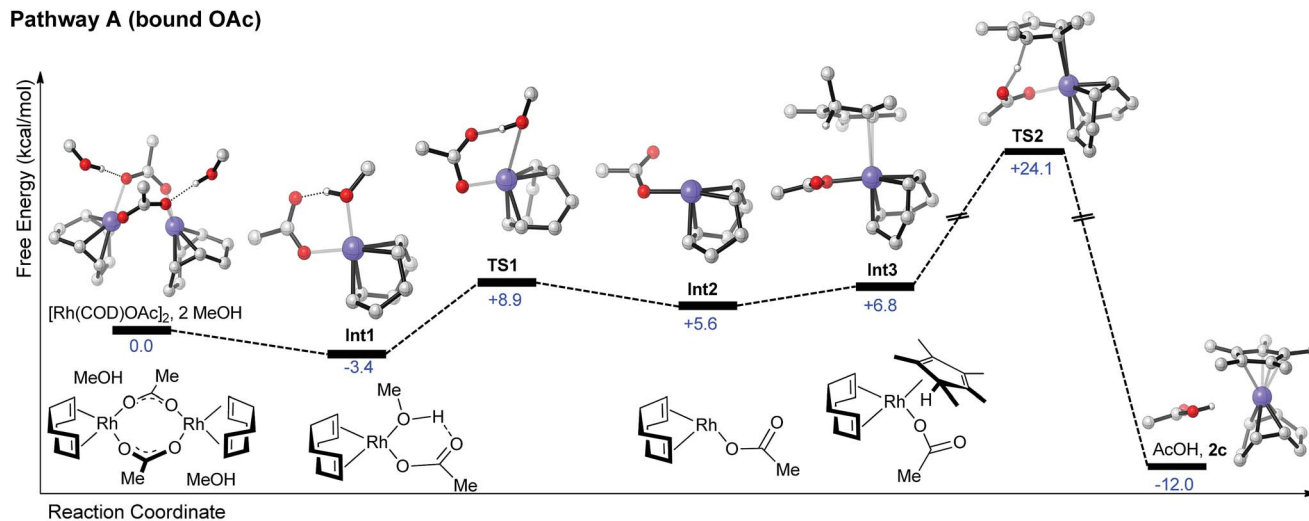
desired complexes (**3a**, **3f-3g**) in good yields. Compared to illustrate examples with rhodium, the complexation is slower with iridium and requires gentle heating. For more reluctant cases, the reaction can be performed with more reactive  $[\text{Ir}(\text{cod})\text{OAc}]_2$ , which is prepared in a single step from  $[\text{Ir}(\text{cod})\text{Cl}]_2$ .<sup>12</sup>

To foster further understanding of the mechanism of complexation, DFT computations (at the PBE0-dDsC/TZ2P//M06/def2-SVP theoretical level, see ESI for computational detail†) of different possible pathways were performed.<sup>13</sup> Two potential pathways exist, which involve reactions of pentamethylcyclopentadiene with either a  $\text{Rh}(\text{OAc})$  (pathway A, Scheme 2) or alternatively a  $\text{Rh}(\text{OMe})$  (pathway B, Scheme 2) fragment. Each pathway begins with the thermodynamically favorable cleavage of the solvated  $\text{Rh}(\text{cod})\text{OAc}$  dimer (as determined from the crystal structure)<sup>14</sup> to form a  $\text{Rh}(\text{cod})(\text{OAc})(\text{MeOH})$  monomer (**Int1**). From this point the two pathways diverge. Methanol can either be directly dissociated in process endergonic process costing  $\sim 12$  kcal mol<sup>-1</sup> (**Int1** → **TS1**, pathway A). **Int2** then forms reaction complex **Int3** in the presence of the Cp\*-

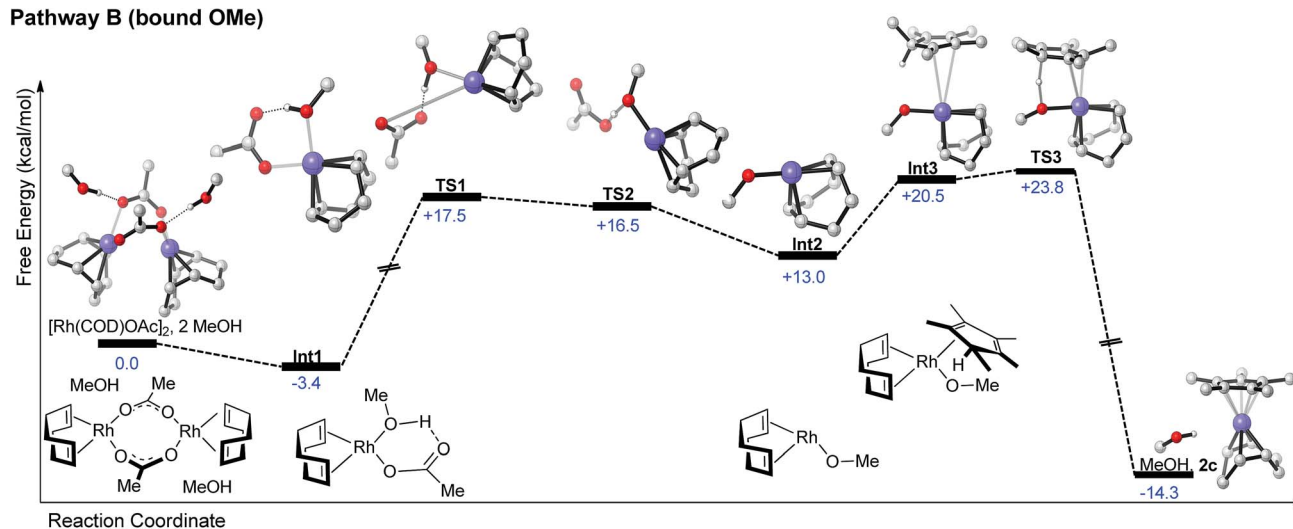
precursor olefin. Proton abstraction from the diene by the bound acetate (**TS2**) is energetically costly and represents the highest point on the pathway A reaction profile at  $+24.1$  kcal mol<sup>-1</sup>. The final products,  $\text{Cp}^*\text{Rh}(\text{cod})$  and acetic acid, are then liberated in an exergonic process. According to the computations, the early parts of pathway A appear to be quite facile, with proton abstraction representing the likely rate-determining step.<sup>13a</sup>

On the other hand, pathway B is characterized by a series of relatively high-energy transition states located at the beginning of the reaction profile (**TS1/TS2**). These costly steps are associated with the initial dissociation of the acetate ion (**TS1**) and proton transfer from methanol (**TS2**) to form a  $\text{Rh}(\text{cod})\text{OMe}$  species (**Int2**) and a liberated acetic acid molecule. Creation of the **Int3** reaction complex by association of the Cp\*-precursor olefin followed by a proton abstraction process (**TS2**) is then accomplished with a low energy barrier and results in direct formation of the  $\text{Cp}^*\text{Rh}(\text{cod})$  product complex and a solvent molecule. Overall, the highest point of both reaction profiles is

### Pathway A (bound OAc)



### Pathway B (bound OMe)



Scheme 2 Potential reaction profiles proceeding from the  $[\text{Rh}(\text{COD})\text{OAc}]_2$  to  $\text{RhCp}^*(\text{COD})$ . Each of the reaction pathways is characterized by roughly similar energetic profiles. Computations at the PBE0-dDsC/TZ2P//M06/def2-SVP level (see ESI for details†).



very close in energy (+24.1 vs. +23.8 kcal mol<sup>-1</sup>) and maybe both accessible under the mild reaction conditions utilized. Since the transformation works cleaner and in higher yields with [Rh(cod)OAc]<sub>2</sub> compared to [Rh(cod)OMe]<sub>2</sub> (which would only allow for pathway B), involvement of pathway A is assumed. Alternatively, the better solubility and potentially easier dimer of [Rh(cod)OAc]<sub>2</sub> may account for the superiority of this precursor complex.

Besides the illustrated practical utility of the complexation strategy, our method offers two significant additional advances. First, it enables new opportunities in complex ligand design previously unfeasible substitutions. Secondly, the facile complexation allows for the first time true *in situ* complexation and catalysis. In our attempt to pursue the concept of late-stage diversification and adjustability of the steric demand of a common ligand platform, we found that deprotonation of Cp<sup>x</sup>H with BuLi and subsequent trapping with TMSCl uniformly provided a single regio- and diastereomer (Scheme 3). X-Ray crystal structure analysis of intermediate **1m** confirmed that the TMS group occupies the position off the C<sub>2</sub>-symmetry axis of **1a** at the more accessible face (See ESI†).<sup>15</sup>

However, complexation of non-C<sub>2</sub>-symmetric ligands poses inherent selectivity issue due to a notoriously difficult facial discrimination in the complexation step of the flat Cp anion.<sup>7d</sup> In consequence, the typical thallium ethoxide complexation method is not suitable due to its lack of facial discrimination of the deprotonation. This results in inseparable mixture of diastereoisomers. Along the same lines, chloride containing rhodium<sup>III</sup> salts mainly resulted in desilylated complexation product.<sup>16</sup> We reasoned that with previously developed complexation method, the rhodium precursor would selectively approach from the face opposed to the TMS group. Indeed, the combination of [Rh(cod)OAc]<sub>2</sub> as metal precursor in *t*BuOH as solvent cleanly yields the desired trimethylsilyl-bearing Cp<sup>x</sup> complexes **2m–2o** as single diastereoisomers (Scheme 4). Similarly, the same method is applicable to access the corresponding iridium complexes **3m–3o**. No proto-desilylated complexes (**3a**, **3f–3g**) were observed. Interestingly, despite the increased steric bulk of the TMS-cyclopentadienes, the complexations proceed at ambient temperature, pointing to a low energy barrier. Both, the regioselectivity of the silylation reaction of the parent chiral cyclopentadiene and the subsequent diastereoselective complexation were unequivocally confirmed by single crystal X-ray diffraction analysis of iridium complexes **3m** and **3o** (Fig. 2).<sup>17</sup>



Scheme 3 Regio- and diastereoselective silylation yields trisubstituted Cp<sup>x</sup> ligands **1m–1o**.



Scheme 4 Diastereoselective complexation with TMS-Cp<sup>x</sup> ligands: 0.1 mmol **1y**, 0.06 mmol [Rh(cod)OAc]<sub>2</sub>, toluene/*t*BuOH, at 23 °C for 3 h. (a) With [Ir(cod)OMe]<sub>2</sub> (b) with [Ir(cod)OAc]<sub>2</sub>.

The proximity of the bulky trimethylsilyl group to the steering pseudoaxial methyl group of **3m** leads to extended side-walls. Comparison of the X-ray crystal structures of **3a**<sup>5i</sup> and **3m** visualizes well the enhanced shielding caused by the installed ligand feature (Fig. 2). While the TMS group slightly influences the chiral backbone, it has a profound effect on the orientation of alkene ligands on the metal (axis with respect to the chiral selector backbone). Consequently, on a substrate bound to the metal, the small fragment (*R*<sub>small</sub>) would minimize the interactions with the TMS function, while the bulkier part (*R*<sub>large</sub>) would stay in the open area of the Cp<sup>x</sup>. The bulk of the silyl group forces an orientation closer to the chiral selector which

a) Schematic enantioselection model



b) Overlay of the X-ray crystal structures of **3a/3m** and **3g/3o**



Fig. 2 Overlay of the X-ray crystal structures reveals the influence of the TMS group on the axis of the olefin ligands (faint blue: parent Cp<sup>x</sup>-complexes without TMS group).



could result in an enhanced interaction and improved discrimination. Hence, the introduction of the TMS as extended side wall could help pre-organization around the metal center thus improving enantio- and regioselectivity compared to the parent ligand.

The performance of complex **2m** was benchmarked in the enantioselective dihydroisoquinolinone synthesis.<sup>18</sup> Compared to the previously best performing catalyst (having the diphenyl acetal which is cumbersome to access), an equivalent selectivity was obtained for styrene as the coupling partners (Scheme 5). Dihydroisoquinolinone **6b**, a precursor for chiral 1,3,2-diazaphospholones,<sup>19</sup> was obtained in 80% yield with high 93 : 7 er. Importantly, a significant selectivity improvement was observed in reactions with challenging cyclic olefins. Complex **2m** outperformed all previously reported complexes.<sup>4f,7d</sup> Reaction with 1,3-cyclohexadiene afforded **6c** in 95 : 5 er (91.5 : 8.5 previously). Similarly, reactions with cyclopentene and dihydrofuran gave **6d** (95 : 5 er) and **6e** (97 : 3 er) in significantly improved enantioselectivity. Notably, norbornene reacted with an excellent selectivity of 99 : 1 er, outperforming Perekalin's planar chiral catalyst.<sup>20</sup> Importantly, the selectivity improved as well for challenging vinyltrimethylsilane (90 : 10 er), while maintaining a similar level of regioselectivity. Even with the new catalytic system, terminal alkyl alkenes remain notoriously challenging substrates. Notably a regioselectivity of 2.4 : 1 was observed, while previously a 1 : 1 mixture was generated.<sup>21</sup> It seems likely that with further fine-tuning of this bulky trisubstituted Cp<sup>x</sup> ligand class, regio- and enantioselectivities could be further boosted.



Scheme 5 Conditions: 0.1 mmol **4**, 0.2 mmol **5**, 5  $\mu\text{mol}$  **2m**, 5  $\mu\text{mol}$   $(\text{BzO})_2$  in EtOH (1 M) at 23 °C.

The development of protocols for an *in situ* complexation, meaning the addition of the Cp<sup>x</sup>H ligand (or a suitable surrogate) and the metal salt altogether with the substrates and additives for the desired catalysis is a high priority, due to its simplicity and accessibility to non-specialists. The outlined complexation has several advantageous characteristics. It proceeds sufficiently fast in almost quantitative manner under mild conditions. The only generated by-products are either catalytic amounts of alcohols (common solvents) or carboxylic acids. In particular for rhodium(III)-catalyzed functionalizations, carboxylic acids or carboxylates are frequently added additives that are essential for reactivity.<sup>22</sup> We examined four different bench-mark reactions for their *in situ* complexation suitability (Scheme 6). For instance, the enantioselective formation of dihydroisoquinolone **6a** by the *in situ* approach proceeded in comparable yield and enantioselectivity compared to the usage of the preformed Cp<sup>x</sup>-rhodium catalyst.<sup>4f</sup> In a similar manner, the *in situ* complexation with the BINOL-OiPr Cp<sup>x</sup> **1h**, follow by the oxidation to Rh(III), allows the synthesis of insoindolone **8**.<sup>10a</sup> Besides substrates with internal oxidants, we investigated the compatibility of common oxidants such as  $\text{Ag}_2\text{CO}_3$  and  $\text{Cu}(\text{OAc})_2$ . In this respect, the desymmetrization of phosphinamide **9** proceeded smoothly.<sup>23</sup> Replacing the common  $[\text{Rh}(\text{cod})\text{OAc}]_2$  by  $[\text{Rh}(\text{cod})\text{OBz}]_2$  did not influence the assembly of the catalyst but is essential for obtaining high enantioselectivity. Moreover, the cyclooctadiene of  $[\text{Rh}(\text{cod})\text{OAc}]_2$  the can be replaced by two ethylene groups ( $[\text{Rh}(\text{C}_2\text{H}_4)_2\text{OAc}]_2$ ). This resulted in a more reactive catalyst for You's reaction of pyrazolone **11** with diphenyl acetylene.<sup>24</sup> Again, the *in situ* method provided comparable results.



Scheme 6 Application of *in situ* Cp<sup>x</sup>-Rh-catalyst assembly under different benchmark reactions. Ar = 3,5- $\text{CF}_3$ - $\text{C}_6\text{H}_3$ , R = CH(iPr)<sub>2</sub>.



## Conclusions

In summary, we disclosed a convenient and general complexation method to access chiral Cp<sup>x</sup> iridium and rhodium complexes. The method has large advance over previous methods as it uses the free Cp<sup>x</sup>H in combination with stable and commercial rhodium(i) and iridium(i) salts without the addition of base or any additive. Moreover, the conditions are mild and the reactions can be conducted without precautions to exclude air and moisture. DFT-calculations revealed two potential pathways with a low energy barrier in which either a bound methoxide or acetate is involved in an intramolecular proton abstraction of the coordinated cyclopentadiene. Moreover, the selectivity and mildness of the complexation method enabled the development of new TMS-containing Cp<sup>x</sup> ligands which displayed superior selectivity for benchmarking dihydroisoquinolone synthesis. Another salient feature is its suitability for *in situ* complexation which significantly enhances the user-friendliness of Cp<sup>x</sup> ligands. This holds the potential to open the versatile catalytic application with designer ligands to a broader community.

## Conflicts of interest

There are no conflicts to declare.

## Acknowledgements

This work is supported by the EPFL and the Swiss National Science Foundation (Consolidator Grant No. 157741). M. D. W. thanks Prof. C. Corminboeuf for financial support and access to computational resources. We thank Dr R. Scopelliti and Dr F. Fadaei Tirani for X-Ray crystallographic analysis of compounds **1m**, **3a**, **3m** and **3o**.

## Notes and references

- J. Hartwig, *Organotransition Metal Chemistry: From Bonding to Catalysis*, University Science Books, Sausalito, CA, 2010.
- (a) T. Piou, F. Romanov-Michailidis, M. Romanova-Michaelides, K. E. Jackson, N. Semakul, T. D. Taggart, B. S. Newell, C. D. Rithner, R. S. Paton and T. Rovis, *J. Am. Chem. Soc.*, 2017, **139**, 1296–1310; (b) A. Davis, C. Wang and T. Rovis, *Synlett*, 2015, **26**, 1520–1524; (c) T. Piou and T. Rovis, *J. Am. Chem. Soc.*, 2014, **136**, 11292–11295; (d) T. Piou and T. Rovis, *Nature*, 2015, **527**, 86–90; (e) F. Romanov-Michailidis, K. F. Sedillo, J. M. Neely and T. Rovis, *J. Am. Chem. Soc.*, 2015, **137**, 8892–8895; (f) T. K. Hyster and T. Rovis, *Chem. Commun.*, 2011, **47**, 11846–11848; (g) Y. Shibata and K. Tanaka, *Angew. Chem., Int. Ed.*, 2011, **50**, 10917–10921.
- (a) T. K. Hyster, D. M. Dalton and T. Rovis, *Chem. Sci.*, 2014, **6**, 254–258; (b) T. K. Hyster and T. Rovis, *Chem. Sci.*, 2011, **2**, 1606–1610; (c) J. M. Neely and T. Rovis, *J. Am. Chem. Soc.*, 2014, **136**, 2735–2738; (d) M. D. Wodrich, B. Ye, J. F. Gonthier, C. Corminboeuf and N. Cramer, *Chem.–Eur. J.*, 2014, **20**, 15409–15418.
- T. Piou, F. Romanov-Michailidis, M. A. Ashley, M. Romanova-Michaelides and T. Rovis, *J. Am. Chem. Soc.*, 2018, **140**, 9587–9593.
- (a) C. G. Newton, D. Kossler and N. Cramer, *J. Am. Chem. Soc.*, 2016, **138**, 3935–3941; (b) B. Ye and N. Cramer, *Acc. Chem. Res.*, 2015, **48**, 1308–1318; (c) G. Erker and A. A. H. van der Zeijden, *Angew. Chem., Int. Ed.*, 1990, **29**, 512–514; (d) A. Gutnov, B. Heller, C. Fischer, H.-J. Drexler, A. Spannenberg, B. Sundermann and C. Sundermann, *Angew. Chem., Int. Ed.*, 2004, **43**, 3795–3797; (e) T. K. Hyster, L. Knörr, T. R. Ward and T. Rovis, *Science*, 2012, **338**, 500–503; (f) B. Ye and N. Cramer, *Science*, 2012, **338**, 504–506; (g) D. Kossler and N. Cramer, *J. Am. Chem. Soc.*, 2015, **137**, 12478; (h) G. Song, W. W. N. O and Z. Hou, *J. Am. Chem. Soc.*, 2014, **136**, 12209–12212; (i) M. Dieckmann, Y.-S. Jang and N. Cramer, *Angew. Chem., Int. Ed.*, 2015, **54**, 12149–12152.
- (a) R. Uson, L. A. Oro, J. A. Cabeza, H. E. Bryndza and M. P. Stepro, in *Inorg. Synth.*, John Wiley & Sons, Inc., 2007, pp. 126–130; (b) M. Arthurs, H. K. Al-Daffaee, J. Haslop, G. Kubal, M. D. Pearson, P. Thatcher and E. Curzon, *J. Chem. Soc., Dalton Trans.*, 1987, 2615–2619; (c) B. M. Trost and C. M. Older, *Organometallics*, 2002, **21**, 2544–2546; (d) M. A. Mantell, J. W. Kampf and M. Sanford, *Organometallics*, 2018, **37**, 3240–3242.
- (a) S.-G. Wang, S. H. Park and N. Cramer, *Angew. Chem., Int. Ed.*, 2018, **57**, 5459–5462; (b) B. Ye and N. Cramer, *J. Am. Chem. Soc.*, 2013, **135**, 636–639; (c) J. Zheng, W.-J. Cui, C. Zheng and S.-L. You, *J. Am. Chem. Soc.*, 2016, **138**, 5242–5245; (d) Z.-J. Jia, C. Merten, R. Gontla, C. G. Daniliuc, A. P. Antonchick and H. Waldmann, *Angew. Chem., Int. Ed.*, 2017, **56**, 2429–2434.
- (a) W.-H. Wang, Y. Suna, Y. Himeda, J. T. Muckerman and E. Fujita, *Dalton Trans.*, 2013, **42**, 9628–9636; (b) S. Yoshizaki, Y. Shibata and K. Tanaka, *Angew. Chem., Int. Ed.*, 2017, **56**, 3590–3593.
- G. Smits, B. Audic, M. D. Wodrich, C. Corminboeuf and N. Cramer, *Chem. Sci.*, 2017, **8**, 7174–7179.
- (a) B. Ye, P. A. Donets and N. Cramer, *Angew. Chem., Int. Ed.*, 2014, **53**, 507–511; (b) B. Ye and N. Cramer, *Angew. Chem., Int. Ed.*, 2014, **53**, 7896–7899; (c) Y.-S. Jang, M. Dieckmann and N. Cramer, *Angew. Chem., Int. Ed.*, 2017, **56**, 15088–15092; (d) T. J. Potter, D. N. Kamber, B. Q. Mercado and J. A. Ellman, *ACS Catal.*, 2017, **7**, 150–153; (e) J. Zheng and S.-L. You, *Angew. Chem., Int. Ed.*, 2014, **53**, 13244–13247; (f) J. Zheng, S.-B. Wang, C. Zheng and S.-L. You, *J. Am. Chem. Soc.*, 2015, **137**, 4880–4883.
- Y. Sun and N. Cramer, *Chem. Sci.*, 2018, **9**, 2981–2985.
- R. N. Haszeldine, R. J. Lunt and R. V. Parish, *J. Chem. Soc. A*, 1971, 3696–3698.
- (a) J. E. Bercaw, N. Hazari and J. A. Labinger, *Organometallics*, 2009, **28**, 5489–5492; (b) T. S. Ahmed, I. A. Tonks, J. A. Labinger and J. E. Bercaw, *Organometallics*, 2013, **32**, 3322–3326.
- C. M. Filloux and T. Rovis, *J. Am. Chem. Soc.*, 2015, **137**, 508–517.
- H.-L. Teng, Y. Luo, B. Wang, L. Zhang, M. Nishiura and Z. Hou, *Angew. Chem., Int. Ed.*, 2016, **55**, 15406–15410.



- 16 (a) J. A. Klang and D. B. Collum, *Organometallics*, 1988, 7, 1532–1537; (b) C. H. Winter, S. Pirzad, D. D. Graf, D. H. Cao and M. J. Heeg, *Inorg. Chem.*, 1993, 32, 3654–3659.
- 17 CCDC 1869889 (**3a**), CCDC 1869894 (**1m**), CCDC 1869888 (**3m**) and CCDC 1869893 (**3o**) contains the supplementary crystallographic data for this paper.†
- 18 N. Guimond, S. I. Gorelsky and K. Fagnou, *J. Am. Chem. Soc.*, 2011, 133, 6449–6457.
- 19 S. Miaskiewicz, J. H. Reed, P. A. Donets, C. C. Oliveira and N. Cramer, *Angew. Chem., Int. Ed.*, 2018, 57, 4039–4042.
- 20 E. A. Trifonova, N. M. Ankudinov, A. A. Mikhaylov, D. A. Chusov, Y. V. Nelyubina and D. S. Perekalin, *Angew. Chem., Int. Ed.*, 2018, 57, 7714–7718.
- 21 B. Ye, PhD thesis, Ecole Polytechnique Fédérale de Lausanne, 2015.
- 22 Recent examples: (a) S. Wu, X. Wu, C. Fu and S. Ma, *Org. Lett.*, 2018, 20, 2831–2834; (b) F. Xu, W.-F. Kang, Y. Wang, C.-S. Liu, J.-Y. Tian, R.-R. Zhao and M. Du, *Org. Lett.*, 2018, 20, 3245–3249; (c) Y. Li, D. Shi, Y. Tang, X. He and S. Xu, *J. Org. Chem.*, 2018, 83, 9464–9470.
- 23 Y. Sun and N. Cramer, *Angew. Chem., Int. Ed.*, 2017, 56, 364–367.
- 24 J. Zheng, S.-B. Wang, C. Zheng and S.-L. You, *Angew. Chem., Int. Ed.*, 2017, 56, 4540–4544.

